Supplementary Information for

Multiple Equilibria in a Land-Atmosphere Coupled System

Dongdong LI [1] (李冬冬), Yongli HE [1] (何永利), Jianping HUANG [1*] (黄建平), Lu BI [1] (秘鲁), and Lei DING [1] (丁磊)

1 *Key Laboratory for Semi-Arid Climate Change of the Ministry of Education, College of Atmospheric Sciences, Lanzhou University, Lanzhou* 730000

Submitted to *Journal of Meteorological Research*

(Submitted January 11, 2018; Accepted July 19, 2018)

[*]Corresponding author: hjp@lzu.edu.cn. Tel: +86 9318914282; Fax: +86 9318914279.

1. Equilibrium solutions and their stability

The solution of the Eqs. (A.19) is

$$[\psi_2, \theta_2, \psi_3, \theta_3]^T = [E_1/G, E_2/G, E_3/G, E_4/G]^T, \tag{S.1}$$

where

$$G = \det\begin{bmatrix} -B_1 & B_1 & -cn^2\psi_1 + \beta n & -cn^2\theta_1 \\ cn^2\psi_1 - \beta n & cn^2\theta_1 & -B_1 & B_1 \\ B_1\sigma' & D_1 - B_2 & cA_1\theta_1 & -cA_2\psi_1 + \beta n\sigma' \\ -cA_1\theta_1 & cA_2\psi_1 - \beta n\sigma' & B_1\sigma' & D_1 - B_2 \end{bmatrix}, \tag{S.2}$$

$$E_1 = \det\begin{bmatrix} 0 & B_1 & -cn^2\psi_1 + \beta n & -cn^2\theta_1 \\ c\tilde{h}(\psi_1 - \theta_1) & cn^2\theta_1 & -B_1 & B_1 \\ 0 & D_1 - B_2 & cA_1\theta_1 & -cA_2\psi_1 + \beta n\sigma' \\ -c\sigma'\tilde{h}(\psi_1 - \theta_1) & cA_2\psi_1 - \beta n\sigma' & B_1\sigma' & D_1 - B_2 \end{bmatrix}, \tag{S.3}$$

$$E_2 = \det\begin{bmatrix} -B_1 & 0 & -cn^2\psi_1 + \beta n & -cn^2\theta_1 \\ cn^2\psi_1 - \beta n & c\tilde{h}(\psi_1 - \theta_1) & -B_1 & B_1 \\ B_1\sigma' & 0 & cA_1\theta_1 & -cA_2\psi_1 + \beta n\sigma' \\ -cA_1\theta_1 & -c\sigma'\tilde{h}(\psi_1 - \theta_1) & B_1\sigma' & D_1 - B_2 \end{bmatrix}, \tag{S.4}$$

$$E_3 = \det\begin{bmatrix} -B_1 & B_1 & 0 & -cn^2\theta_1 \\ cn^2\psi_1 - \beta n & cn^2\theta_1 & c\tilde{h}(\psi_1 - \theta_1) & B_1 \\ B_1\sigma' & D_1 - B_2 & 0 & -cA_2\psi_1 + \beta n\sigma' \\ -cA_1\theta_1 & cA_2\psi_1 - \beta n\sigma' & -c\sigma'\tilde{h}(\psi_1 - \theta_1) & D_1 - B_2 \end{bmatrix}, \tag{S.5}$$

$$E_4 = \det\begin{bmatrix} -B_1 & B_1 & -cn^2\psi_1 + \beta n & 0 \\ cn^2\psi_1 - \beta n & cn^2\theta_1 & -B_1 & c\tilde{h}(\psi_1 - \theta_1) \\ B_1\sigma' & D_1 - B_2 & cA_1\theta_1 & 0 \\ -cA_1\theta_1 & cA_2\psi_1 - \beta n\sigma' & B_1\sigma' & -c\sigma'\tilde{h}(\psi_1 - \theta_1) \end{bmatrix}, \tag{S.6}$$

are function of ψ_1 and θ_1. Using this solution, Eqs. (A.11) and (A.18) become

$$-k(\psi_1 - \theta_1) + c\tilde{h}(E_3 - E_4)/G = 0, \tag{S.7}$$

$$c(E_1E_4 - E_2E_3)/G^2 + [(D_1 - 2k'\sigma')\theta_1 + D_2] = 0, \tag{S.8}$$

two nonlinear equations in the two variables ψ_1 and θ_1. It's easy to find that if we set $\tilde{h} = 0$, all values of (E_1, E_2, E_3, E_4) equal to zero, thus wave amplitudes $(\psi_2, \theta_2, \psi_3, \theta_3)$ equal to zero, then we can only obtain Hadley circulation solution. Therefore, no topography, no

multiple equilibria.

The linear perturbation equation that determine the stability of the equilibrium solution is given in what follows.

The linear perturbation equations that determine the stability of the equilibrium solution is

$$\begin{vmatrix}
-(k+\alpha) & 0 & c\tilde{h} & k & 0 & -c\tilde{h} & 0 & 0 & 0 \\
-\frac{cn^2\bar{\psi}_3}{n^2+1} & -(k+\alpha) & \frac{\beta n - cn^2\bar{\psi}_1}{n^2+1} & -\frac{cn^2\bar{\theta}_3}{n^2+1} & k & -\frac{cn^2\bar{\theta}_1}{n^2+1} & 0 & 0 & 0 \\
\frac{c(n^2\bar{\psi}_2-\tilde{h})}{n^2+1} & \frac{cn^2\bar{\psi}_1-\beta n}{n^2+1} & -(k+\alpha) & \frac{c(n^2\bar{\theta}_2+\tilde{h})}{n^2+1} & \frac{cn^2\bar{\theta}_1}{n^2+1} & k & 0 & 0 & 0 \\
k\sigma' & c\bar{\theta}_3 & -c(\bar{\theta}_2+\sigma'\tilde{h}) & -[B_3+d_1+C_1\alpha] & -c\bar{\psi}_3 & c(\bar{\psi}_2+\sigma'\tilde{h}) & d_2 & 0 & 0 \\
-\frac{cA_2\bar{\theta}_3}{n^2+1} & k\sigma' & \frac{cA_1\bar{\theta}_1}{n^2+1} & \frac{cA_1\bar{\psi}_3}{n^2+1} & -(\frac{B_2+d_1}{n^2+1}+C_2\alpha) & \frac{\beta n\sigma' - cA_2\bar{\psi}_1}{n^2+1} & 0 & \frac{d_2}{n^2+1} & 0 \\
\frac{c(A_2\bar{\theta}_2+\sigma'\tilde{h})}{n^2+1} & -\frac{cA_1\bar{\theta}_1}{n^2+1} & k\sigma' & -\frac{c(A_1\bar{\psi}_2+\sigma'\tilde{h})}{n^2+1} & \frac{cA_2\bar{\psi}_1-\beta n\sigma'}{n^2+1} & -(\frac{B_2+d_1}{n^2+1}+C_2\alpha) & 0 & 0 & \frac{d_2}{n^2+1} \\
0 & 0 & 0 & d_4 & 0 & 0 & -(d_3+\alpha) & 0 & 0 \\
0 & 0 & 0 & 0 & d_4 & 0 & 0 & -(d_3+\alpha) & 0 \\
0 & 0 & 0 & 0 & 0 & d_4 & 0 & 0 & -(d_3+\alpha)
\end{vmatrix} = 0 . \qquad \text{(S.9)}$$

2. Equilibrium states of higher order spectral models

We choose eight eigenfunctions (see (S.10)) for the truncated spectral model. In the main body, all of the equilibrium solutions are obtained from the 9-component system (using three eigenfunctions, $F_i, i=1,2,3$). Here, we give the equilibrium solutions of 18-component system (using six eigenfunctions, $F_i, i=1,2,3,...,6$) and 24-component (using eight eigenfunctions, $F_i, i=1,2,3,...,8$) . The equilibrium solutions are obtained by numerical integration, using a second-order Heun method with a fixed time step $\Delta t=0.01$ time units. One of the equilibrium states for the 18-component system and the 24-component system are illustrated in Fig. S1 and S2, respectively. Note that the numerical integration method is not easy to find all equilibrium solutions, we may obtain just one of the equilibrium solutions of the 18-component or the 24-component system.

$$\left.\begin{aligned} F_1 &= \sqrt{2}\cos(y) \\ F_2 &= 2\cos(nx)\sin(y) \\ F_3 &= 2\sin(nx)\sin(y) \\ F_4 &= \sqrt{2}\cos(2y) \\ F_5 &= 2\cos(nx)\sin(2y) \\ F_6 &= 2\sin(nx)\sin(2y) \\ F_7 &= 2\cos(2nx)\sin(y) \\ F_8 &= 2\sin(2nx)\sin(y) \end{aligned}\right\} \qquad \text{(S.10)}$$

Compare the Fig. S1, S2 with the Fig. 1, 2, we find that the flow patterns of the equilibrium states in 9-component, 18-component and 24-component systems are obviously different from each other. Fig. S1 shows a meridionally dipole flow patterns. Fig. S2 shows that the blocking-like anticyclones are simultaneously located to the west side and east side of the mountains. Therefore, the flow patterns of the equilibrium states are sensitive to the horizontal resolution of the model.

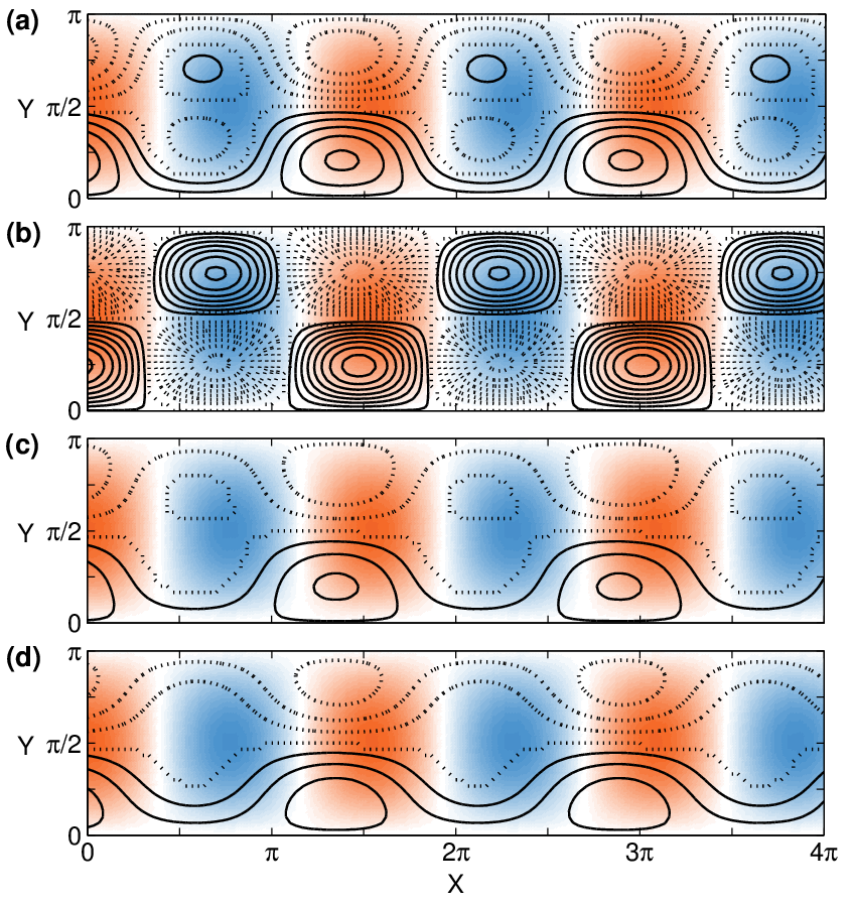

Fig. S1. One of the equilibrium states of the 18-component system, with $m = 3.7$ at $C_g = 55$ W m^{-2}. (a, b) The streamfunction fields of the upper and lower layers, respectively. (c, d) The temperature fields of the atmosphere and the land, respectively. The zero and negative contours are dashed. The contour intervals (CI) and ranges (R) are: (a) $CI = 1.0\times10^7$, $R = (-4,5)\times10^7$ m^2 s^{-1}; (b) $CI = 1.0\times10^6$, $R = (-8,8)\times10^6$ m^2 s^{-1}; (c) $CI = 5$, $R = (-10,15)$ K; (d) $CI = 5$, $R = (-15,15)$ K. The colored background shows the topographic heights in the model, and the warm (cool) tones indicate positive (negative) regions.

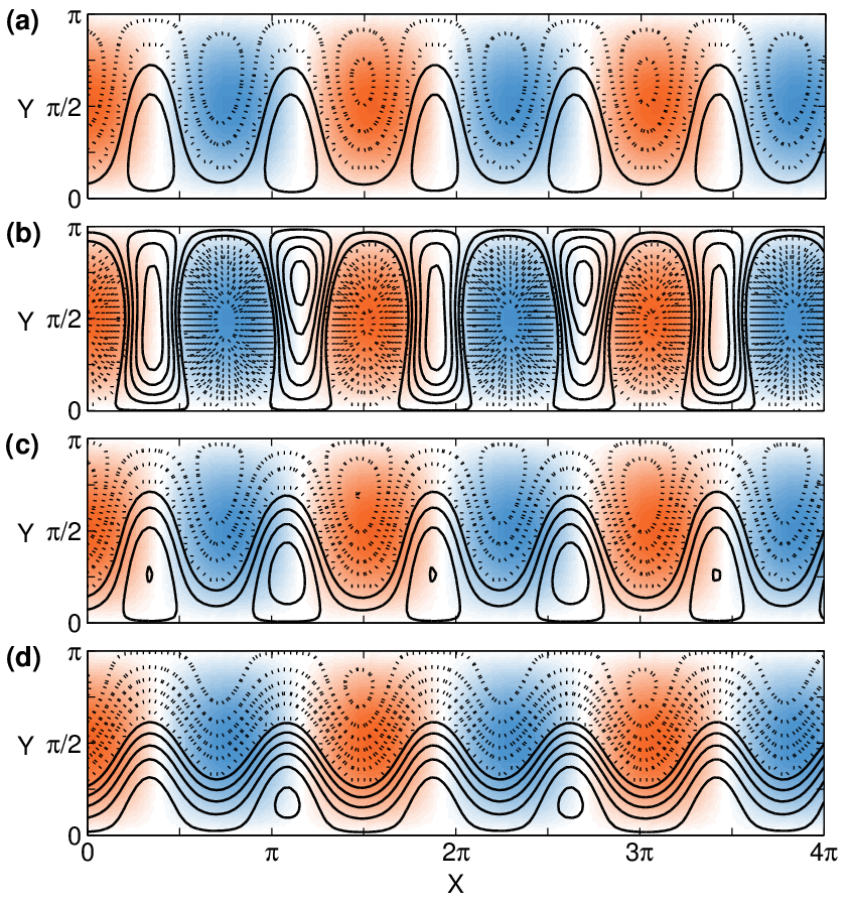

Fig. S2. Same as Fig. S1, but for one of the equilibrium states of the 24-component system. The CI and R are: (a) $CI = 1.0\times10^{7}$, $R = (-3, 2)\times10^{7}$ $\mathrm{m^2\,s^{-1}}$; (b) $CI = 1.0\times10^{6}$, $R = (-10, 6)\times10^{6}$ $\mathrm{m^2\,s^{-1}}$; (c) $CI = 2$, $R = (-10, 8)$ K; (d) $CI = 2$, $R = (-12, 12)$ K.

3. An observational evidence for the trough-type and ridge-type equilibria

In the main body, we have shown that there may be multiple wave phase equilibria associated with the trough-type and ridge-type driven by the topography. Do there truly exist two types of quasi-stationary planetary wave with distinct wave phase relative to the topography in the real atmosphere? Our answer is yes. For example, as shown in Fig. S3, there was the anomalous large-amplitude trough over the Ural region (blue box, 50~70N, 40~80E) in January 1997; however, in January 2012, there was the anomalous large-amplitude ridge over the Ural region. Our future study is to check more results of the simple truncated model with the observations.

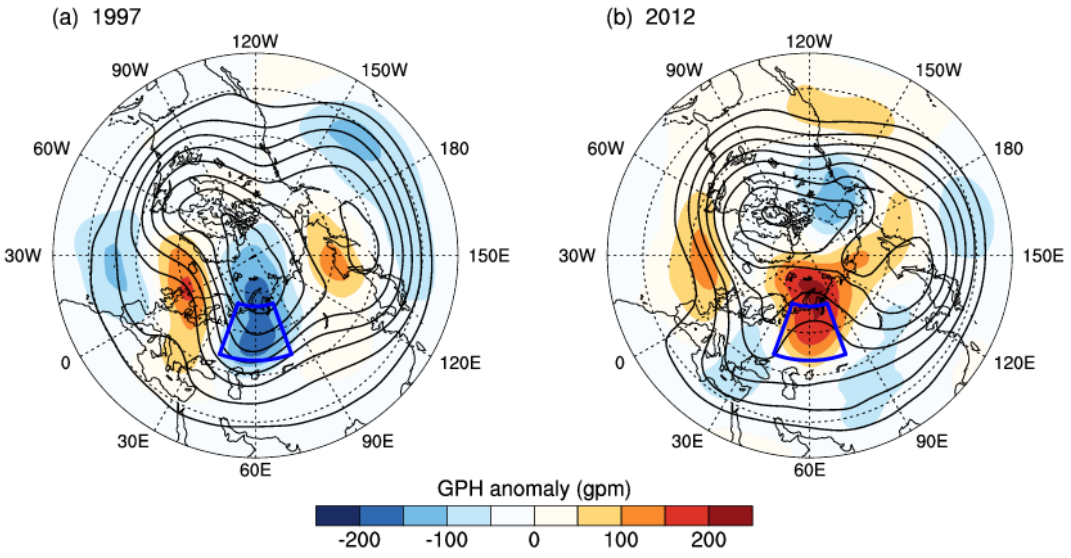

Fig. S3. Monthly mean geopotential height at 500 hPa (black solid contours) and its deviation from the climatological (1981-2010) mean (shaded) in (a) January 1997, (b) January 2012. Contour interval 100 gpm for full fields, 50 gpm for anomalies. The data is derived from the NCEP-NCAR reanalysis data on a 2.5 degree x 2.5 degree grids (https://www.esrl.noaa.gov/psd/data/gridded/data.ncep.reanalysis.pressure.html).